Musical Applications of Electric Field Sensing

Joseph A. Paradiso and Neil Gershenfeld

Physics and Media Group
MIT Media Laboratory
Cambridge, MA 02139

joep,gersh@media.mit.edu

ABSTRACT

The Theremin was one of the first electronic musical instruments, yet it provides a degree of expressive real-time control that remains lacking in most modern electronic music interfaces. Underlying the deceptively simple capacitance measurement used by it and its descendants are a number of surprisingly interesting current transport mechanisms that can be used to inexpensively, unobtrusively, robustly, and remotely detect the position of people and objects. We review the relevant physics, describe appropriate measurement instrumentation, and discuss applications that began with capturing virtuosic performance gesture on traditional stringed instruments and evolved into the design of new musical interfaces.

1) Introduction

The essence of musical expression lies in manipulation. A great musical instrument provides the player with many continuous control degrees of freedom that can be shaped to communicate musical intent. The design of mature acoustic instruments has evolved over centuries (if not millennia) to blend these relevant controls into a compact interface that matches the sensory and motor capabilities of the musician (roughly, millimeter resolution in space and millisecond resolution in time). The performance interface can, and should, be evaluated as any engineered transducer is: are the resolution, dynamic range, degrees of freedom, hysteresis, and signal-to-noise ratio adequate? Unfortunately, for most common electronic instruments, the answer is an easy no; the seven bits of velocity resolution plus the set of thumbwheels in an ordinary keyboard does not come close to capturing what a performer can express.

The Theremin was the first truly responsive electronic musical instrument, and few things since have matched the nuance in Clara Rockmore's lyrical dynamics on this essentially monotimbral, monophonic device [Moog 1994; Rockmore 1987]. It used a simple capacitance measurement to sense the proximity of the player's hands. This implementation is best understood as an early and important example of a broader class of techniques, termed "electric field sensing". Capacitance is a quantity describing the charge stored between a set of electrodes. More generally, it is possible to use multiple electrodes to create electric fields, then measure the induced potentials and displacement currents in order to inexpensively, remotely, and robustly learn about the intervening distribution of

Draft 1.9, April 1996; to be published in *Computer Music Journal*

matter. This article will review the history of electric field sensing, examine the underlying physics, and discuss several musical applications that we have implemented at the MIT Media Laboratory[1].

Although capacitive sensing provided the first noncontact interface to an electronic musical instrument, several other sensing channels have been exploited for capturing musical gesture; Roads [1996] gives an excellent summary. Ultrasonic ranging and motion detectors have been used for decades to provide musical response to free gesture [Chabot 1990; Gehlhaar 1991], and are the basis for many interesting musical interfaces developed at STEIM [Anderton 1994]. While they work nicely in many applications, there are several considerations (e.g., no sensitivity past obstructions, narrow beamwidth, limited resolution, long propagation delays, drift and interference from changes in the environment) that can pose difficulty in implementing such musical sonar interfaces. Optical sensors have been used for noncontact interfaces in a variety of musical projects. These range from simple hand trackers using an light-emitting diode (LED) and photodiode [Rich 1991; Fisher and Wilkinson 1995] to systems employing photosensor arrays [Rubine and McAvinney 1990] or video cameras and complicated image processing [Collinge and Parkinson 1988; Wren and Sparacino 1996]. As with sonar, the optical systems are limited in several applications by analogous considerations (e.g. obstructions blocking the line of sight, limited angular range, varying reflectance, effects from background light). Digital vision systems can still be confused by clutter and changes in the environment, although this will certainly improve as more powerful algorithms and processors are developed. Radar and microwave motion sensors havealso been occasionally used to measure the dynamics of musical performers [Mann 1992]. As with our electric field sensors, these devices can sense through nonconducting obstructions, but suffer from hardware complication, limited resolution, sensitivity to clutter, and restrictions on human exposure to electromagnetic radiation. New developments in low-cost micropower ranging radars [Azevedo and McEwan 1996], however, promise to make this sensing channel much more practical and attractive for future musical application.

Electric field sensing provides a means for tracking musical gesture that builds on the strengths of the many alternative technologies described above, while avoiding several of their weaknesses. Its application, however, has thusfar been restricted by limited common understanding of the underlying mechanisms, the required instrumentation, and the flexible modes available for interface design. These topics will be covered in the next sections.

A new sensor for musical instruments is of no use unless the data from it can be gathered, interpreted, and turned into sounds. Fortunately, progress in all these areas is helping foster the acceptance of new controllers. There are new musical [McMillen et al. 1994] and general purpose [Slater 1995] specifications emerging for high-speed networks and interface devices. Practical real-time modeling synthesis techniques [e.g., Smith 1992; Weigend and Gershenfeld 1993] can use (and in fact demand) responsive controllers for their algorithm parameters. Musical software environments are emerging that can meaningfully interpret gestural information, helping virtuosic players control more sounds in more ways, and enabling beginners to engage in creative expression [e.g., Machover 1992; Puckette 1991]. A working controller is still no good unless musicians are interested

[1] See *http://physics.www.media.mit.edu* for audio/visual excerpts from these projects.

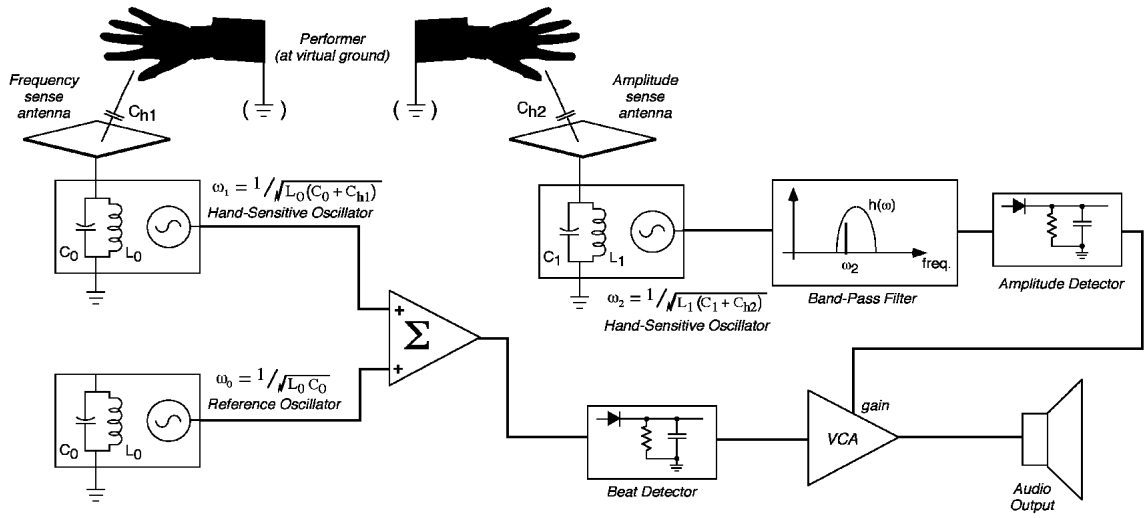

Figure 1: Essential design of the basic Theremin

in it and able to use it. The new projects that we will describe are carefully grounded in the aesthetic sensibility of a performance domain, either building on past practice to bring new degrees of freedom to mature instruments (such as a cello), or inventing wholly new instruments based on experience in other domains (such as that of a magician). This balance between innovation and constraint is crucial in providing an error metric to help guide the creative as well as the technical development of new instruments.

2) Historical Context

Leon Theremin developed his instrument in the early 1920's [Galeyev 1991] while experimenting with contemporary radios and noting the effects of body position on the signals [Martin 1993]. Fig. 1 shows the design of a classic Theremin [Garner 1967; Moog 1996; Simonton 1996]. An antenna external to the Theremin chassis is connected to an "LC" tank oscillator, with frequency determined by the reactance of a network composed of an inductance (L) and capacitance (C). By moving a hand into the vicinity of this sense antenna, the performer's body increases the effective capacitance to ground of the antenna, thus shifting the oscillation frequency (ω_1) of the LC tank. Section 5 will discuss this interaction in more detail and introduce an effective circuit model of the body. As the performer varies the distance of his or her hand from the antenna, the capacitive coupling (and hence ω_1) changes accordingly. Because the capacitance is usually very small (typically below a picofarad), this oscillator must be run well above audio frequencies (typically 100 kHz to 1 MHz) to attain significant coupling and dynamic range. The radio-frequency wavelength is approximately 3 km at 100 kHz, hence most Theremins operate well into the near-field limit and should be analyzed as a slowly-varying electrostatics problem with negligible radiation retardation effects [Jackson 1975]; we will make this approximation throughout this article. The hand-dependent frequency (ω_1) is then down-shifted to audio by mixing the ω_1 signal with a nearby fixed frequency reference (ω_0) and detecting the low frequency beats at ω_0-ω_1. Theremins usually sport a second proximity-variable oscillator/antenna (ω_2) to control the amplitude of the audio; here, this

ω_2 signal is applied to a steep bandpass filter, then the amplitude of its output is detected to determine the gain of a voltage controlled amplifier (VCA) in the audio path. As a hand moves near this volume-control antenna, ω_2 moves into tune with the bandpass filter, changing the audio level through the VCA. Leon Theremin applied this idea in several other inventions, such as the polyphonic Theremin, the Terpsitone (which responded to the body gestures of dancers) and, anticipating the theme of our work described in the following section, an electronic cello [Mattis and Moog 1992].

This general approach of comparing a variable oscillator (whose time constant is set by capacitive coupling to external objects) to a fixed reference frequency is employed in several common proximity-sensing applications, such as "stud finders," which measure the local material density inside walls to determine the location of hidden support structures [Franklin 1978]. Such methods of electric field sensing we class as "loading mode"; i.e., measuring the displacement current pulled from a transmitting electrode. Recent proximity-sensing applications [Vranish 1994] have dispensed with the dual-oscillator Theremin structure, and use feedback amplifiers to directly measure the displacement current (as discussed later; see Figure 15).

Although different applications of capacitive sensing have occasionally appeared in various special performances over the last decades [e.g., Shapiro and Patterson 1972], most incarnations of capacitive measurement for musical applications since the Theremin have been in touch-sensitive keyboards. One of the most refined examples is in the keyboards designed by Moog and collaborators [Moog and Rhea 1990], which used the loading of the fingertips on an array of electrodes at each key to track finger positions after keys were hit. Simpler commercial examples are the touch keyboards packaged with the portable Synthi-AKS analog synthesizer from Electronic Music Systems (EMS) [Vail 1993] and the synthesizers manufactured by Electric Dream Plant (EDP), namely the Wasp and Gnat [Newcomb, 1994]; these trigger notes when a player contacts an insulated plate at each key. Similar capacitive touch sensors were also used with the early Buchla analog synthesizers and musical interfaces [Aikin 1984]. Most touch-keyboard designs sense the capacitive coupling of ambient line frequency through the body, or use the added capacitive loading of a finger on a plate to shift the phase of a clock signal [Lancaster 1988].

The Mathews/Boie radio drum [Mathews 1990] (Fig. 2) also employs a near-field capacitive measurement. Unlike the single-electrode loading-mode designs outlined above, the radio drum determines the capacitance between an active baton (transmitter) and a set of shaped "receive electrodes" in a plane below the baton. The signal broadcast by the baton is synchronously detected at the receivers in order to filter out background noise (suitable circuitry is described in Section 3). A pair of batons can be used, which broadcast and are synchronously detected at different frequencies so that they can be separately tracked. As the performer moves the baton in the sensitive region, the detected signals will vary as a function of the distance (hence capacitive coupling) between the baton and the receive electrodes. By appropriately tapering the receive electrodes and processing the received signals, the 3-D position of the baton can be determined and used to control a synthesizer or conduct a sequenced performance [Mathews 1989].

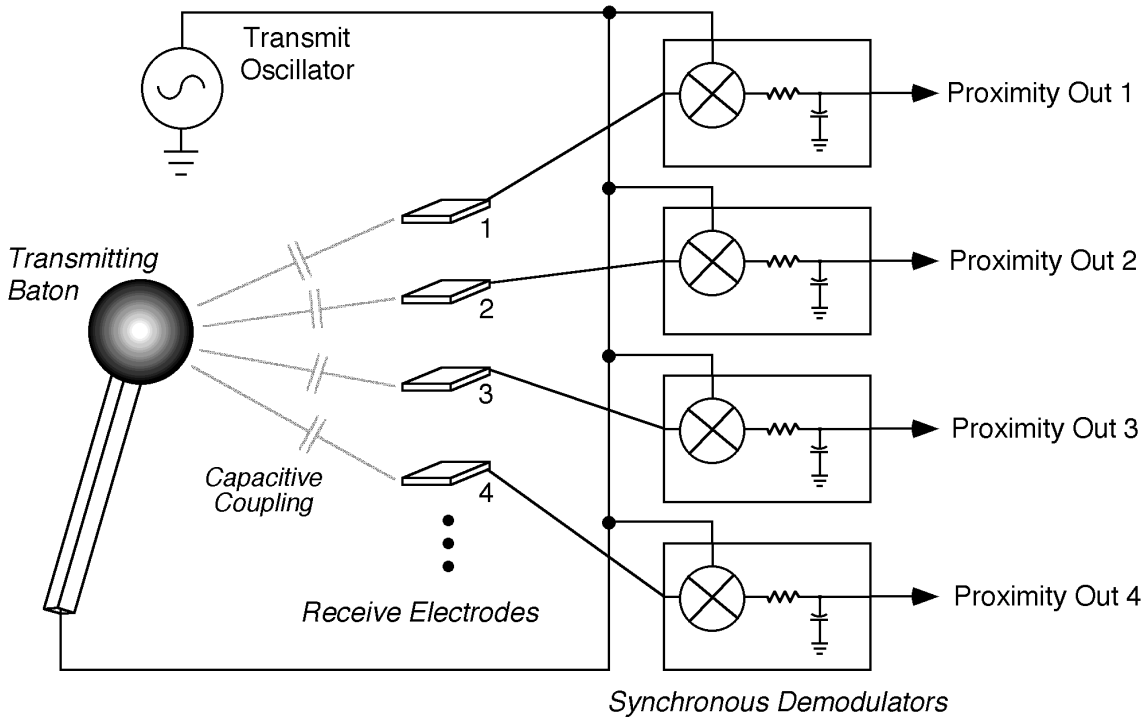

Figure 2: Proximity sensing in the Mathews/Boie Radio Drum

3) Tracking Cello Bows

Together with Joseph Chung, we developed the "hypercello" for Yo-Yo Ma's performance of Tod Machover's composition *Begin Again Again...* [Machover 1991a]. The hypercello sensors measured the player's inputs to the instrument and used them to control a range of sound sources. The goal of the sensing was to unobtrusively and responsively detect the player's actions as he followed notated music. A real-time computing environment mapped the sensor information into sounds, thereby extending classical technique so that gestures controlled notes, phrases, and algorithm parameters.

The cello, a RAAD built in Toronto, Canada by Richard Armin, used PVDF piezoelectric polymer pickups [Duperray 1984] to sense the vibrations of the top plate, which was acoustically floating from a solid body so that little direct sound was radiated. In addition, when pressed, each string contacted a resistive thermoplastic strip (M-411 from Mitech in Twinsburh, Ohio, USA) on the fretboard that sensed the positions of the fingers. The bow-wrist angle was measured using a Exos Wrist Master exoskeleton based on magnets and Hall-effect sensors (Exos Inc., Burlington, Massachusetts, USA), and the bow position and pressure were determined by the system that is discussed below. More information on the other sensors mentioned above was presented in Gershenfeld [1991]. A network of Macintosh computers gathered data from the sensors, processed these data in the Hyperlisp environment [Chung 1988], and controlled samplers, synthesizers, and signal processors to generate the output sounds. A block diagram of the system is shown in Figure 3.

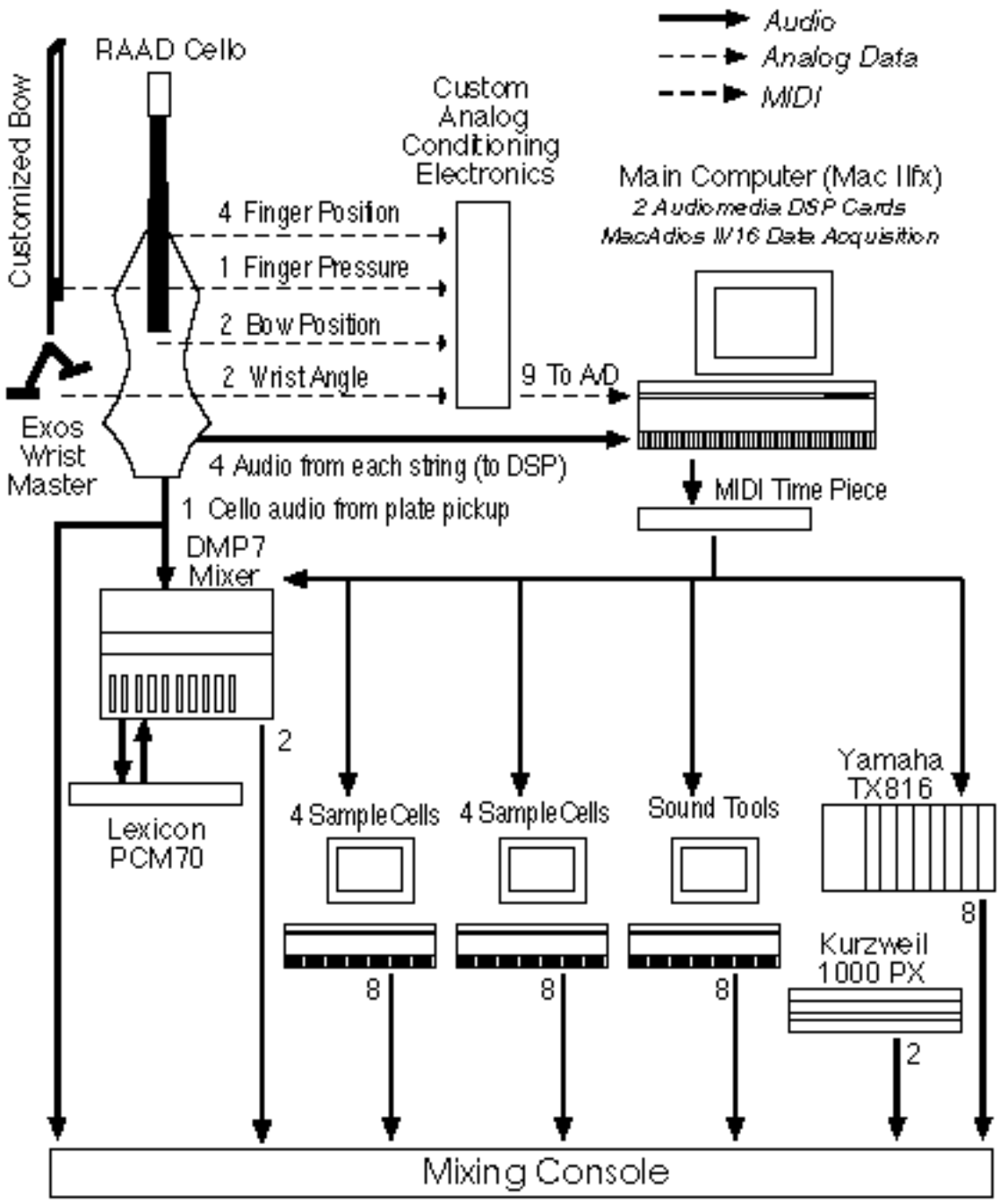

Figure 3: Hypercello system for performance of *Begin Again Again ...*

The most challenging sensing task was measuring the bow position (lateral distance, δx) and placement (longitudinal distance from the bridge, δy). Previous studies have either relied on signal processing to recognize bowed gesture from the audio stream [Nègyesy and Ray 1989; Hong 1992], or employed inertial sensors that have problems with drift and optical techniques that have difficulty maintaining line-of-sight [Chafe 1995]. The radio drum does not require contact between the baton and the planar receiver, but there is not room on the bow or cello for such a large shaped electrode.

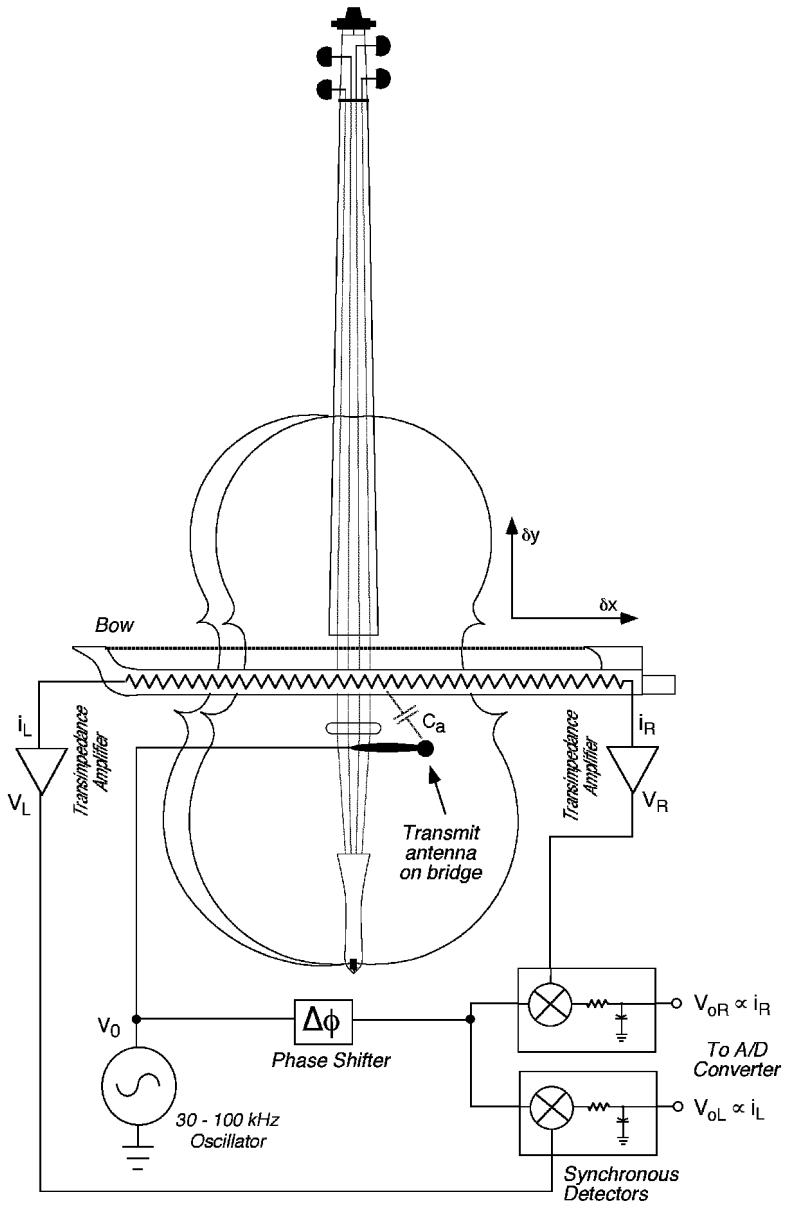

Figure 4: Block diagram of the cello bow position sensing system

We solved these problems by merging the techniques for measuring each coordinate, as shown in Figure 4. Capacitive coupling into a bow electrode measured placement, and making the bow electrode out of a resistive material added a real impedance that varied with position [Gershenfeld 1993]. This geometry gave a useful signal over the full bowing range that was linear and insensitive to bow rotations.

A sine wave of approximately 100 kHz frequency and 20V peak-to-peak amplitude was transmitted from an antenna roughly 5 cm tall mounted behind the bridge, and the strings were grounded to prevent perturbations from the player. The capacitance between this antenna and the bow electrode was generally in the femtofarad (fF) range. The bow electrode was made from a resistive thermoplastic (as above, M-411, having a resistivity of

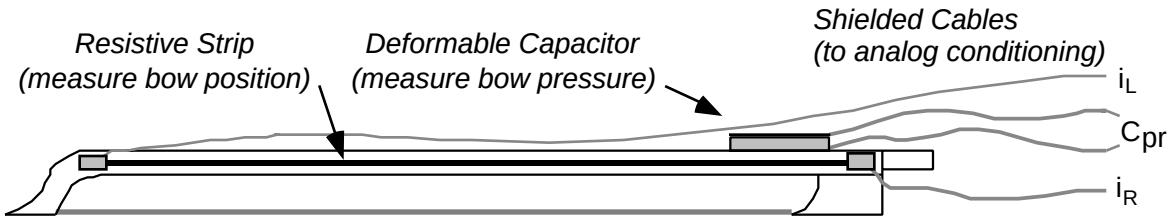

Figure 5: Cello bow equipped with position sensors

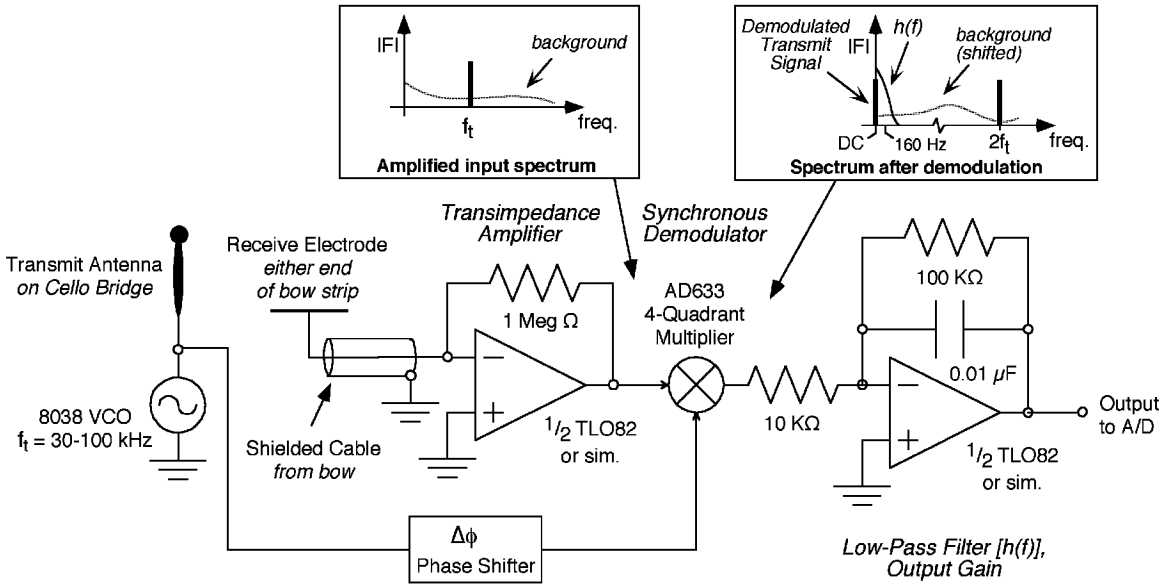

Figure 6: Single channel of synchronously detecting receive electronics

10^{11} Ω-cm), cut into a 5 mm wide strip to give a resistance of a few MΩ and attached to the bow with a laminating tape[2]. Contact to this strip was made at either end by copper tape with an electrically conducting glue[3] and the signals were brought out by fine (47-mil diameter) flexible coaxial cable[4] to maintain electrostatic shielding (Figure 5).

The small (circa 1 μA) displacement currents flowing from each end of the resistive strip need to be separated from potentially much larger background noise (a performance stage can be a hostile electromagnetic environment, with background contributions from lighting circuits, etc.); thus synchronous detection was used. As shown in Figure 6, the shielded coaxial cables were connected to the inputs of conventional JFET-input operational amplifiers (such as the AD712 or TL082) configured as current-to-voltage converters (transimpedance amplifiers). These signals are then 4-quadrant multiplied by the transmitted sine wave, which is phase-shifted to correct for the effects of cable capacitance (and the 90° lead from the capacitive displacement current, which can also be eliminated by using an integrating capacitor in parallel with a bias return resistor for the amplifier

[2] Tape 9449, 3M, St. Paul, MN.

[3] Tape 1181, 3M, St. Paul, MN.

[4] AS 450-3650SR, Cooner, Chatsworth, CA.

feedback network), and then low-pass filtered by a first-order filter with a cut-off of a few hundred Hz (determined by a trade-off between the needed response time and position resolution). This has the effect of creating a narrow band-pass filter centered on the oscillator frequency, with a width determined by the time constant of the output filter (here we set $\delta f/f \approx 1\%$). Viewed in the time domain, the only noise that passes is the small component with frequency and phase close to that of the transmit oscillator. This also allows the front-end amplifier to be run at its optimum frequency for low-noise performance. If the frequency is too low, the $1/j\omega C$ impedance being measured is very large (hence the received current is small) and contributions from 1/f amplifier noise increase, reducing the signal-to-noise ratio. On the other hand, if the frequency is too high, the received amplitude again decreases due to finite front-end amplifier bandwidth, and effects from parasitic cable capacitance become significant. Using the components listed, these considerations dictate an optimal frequency ranging 50-100 kHz. This sensitive circuit, similar to the matched filter in a superheterodyne radio receiver, is simple and inexpensive (below $10 per channel). It can be made even less costly by using a CMOS switch instead of the multiplier, but, unless a bandlimited front-end is used, this can add a small amount of noise that is passed on the harmonics of the switching square wave.

These outputs from the two channels (left- and right-bow) were sampled as 12-bit integers at 100 Hz and analyzed to determine the bow coordinates. The effective circuit is an AC-coupled potentiometer (Figure 7). In terms of these components, the currents at each end (measured by the synchronous amplifiers) are:

$$i_L = V_0 \frac{R_R}{R_L R_R + (R_L + R_R)/(j\omega C_a)} \qquad i_R = V_0 \frac{R_L}{R_L R_R + (R_L + R_R)/(j\omega C_a)} \tag{1}$$

where R_L and R_R are the resistances along the strip from the bridge position to the left and right bow ends, C_a is the capacitance between the resistive strip and antenna, V_0 is the transmitter antenna drive voltage, and ω is the transmit frequency. The normalized current difference:

$$\frac{i_L - i_R}{i_L + i_R} = \frac{R_R - R_L}{R_R + R_L} = \frac{(R_0 + \alpha x) - (R_0 - \alpha x)}{(R_0 + \alpha x) + (R_0 - \alpha x)} = \alpha \frac{x}{R_0} \tag{2}$$

is then independent of the capacitance, and since the resistances are proportional to the lateral displacement x ($R_L = R_0 + \alpha x$ and $R_R = R_0 - \alpha x$, where α is the strip resistance per unit length, R_0 is half the strip resistance, and x=0 at mid-bow), this difference provides an estimate of x. The capacitance C_a falls off as 1/y (y is the distance from the bridge) for small y, because the two electrodes can be approximated as a parallel plate capacitor. It then crosses over to a $1/y^2$ decay at longer distances as the finite size of the electrodes becomes significant and the electrodes can be approximated as a pair of point charges. A numerical calculation of this falloff in C_a with y is shown in Figure 8. Since the capacitive impedance ($\gtrsim 10^7\ \Omega$) is much greater than the real impedance ($\lesssim 10^6\ \Omega$), and parallel-plate coupling dominates over most of the bowing range, the inverse of the total current:

$$\frac{1}{i_R + i_L} = \frac{1}{V_0}\left[\frac{R_L R_R}{R_L + R_R} + \frac{1}{j\omega C_a}\right] \approx \frac{1}{j\omega C_a V_0} \qquad \frac{y}{j\omega V_0} \quad (\textit{for small } y) \tag{3}$$

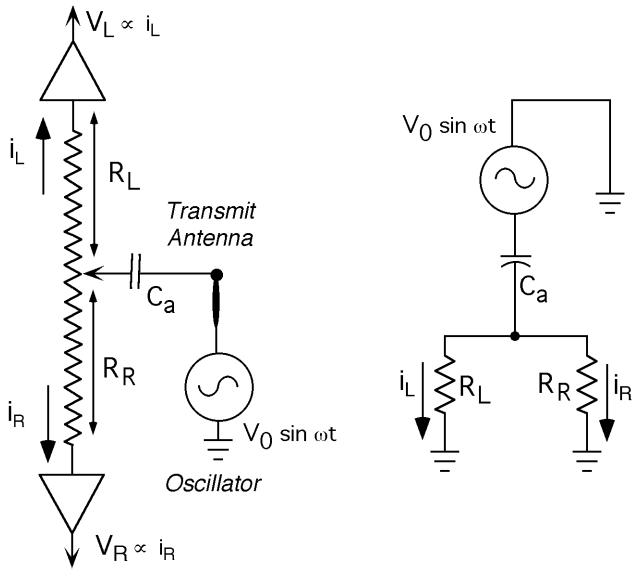

Figure 7: Potentiometer analogy (left) and equivalent circuit (right) for bow receivers

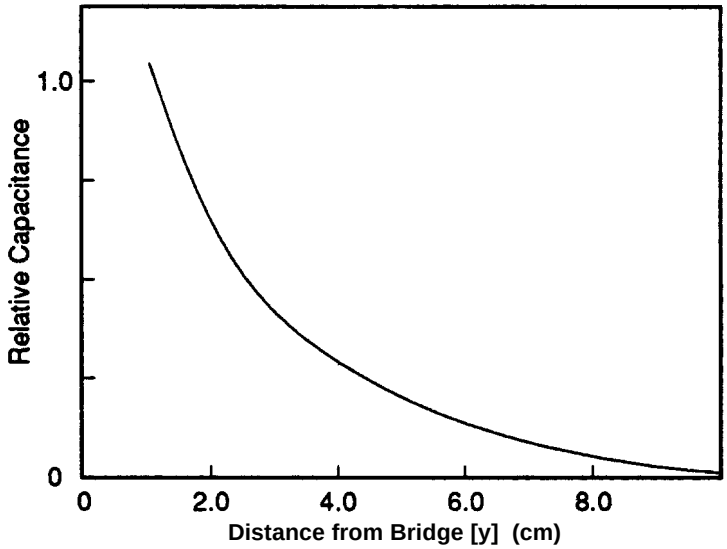

Figure 8: Dependence of net capacitance (C_a) on antenna/bow separation

is approximately proportional to the distance of the bow from the bridge (y) . Therefore, from the sums and differences of the currents from the ends of the bow we can find the position and placement of the bow.

Fig. 9 plots actual data taken from the bow. The top row shows the normalized current difference (Equation 2), and the bottom row shows the inverse sum (Equation 3). In both cases, the vertical coordinates were normalized to the range of bow motion in x and y. The left column shows data for transverse (x) bow strokes at constant y, and the right column shows data for longitudinal (y) bow motion towards and away from the bridge with the bow kept centered at x=0. The decoupling of x and y predicted by Equations 2 and 3 is seen in these plots; any residual deviation is dominated by the orthogonal motion of the bow during the measurements. Over a 50-cm bow stroke, it is possible to resolve a

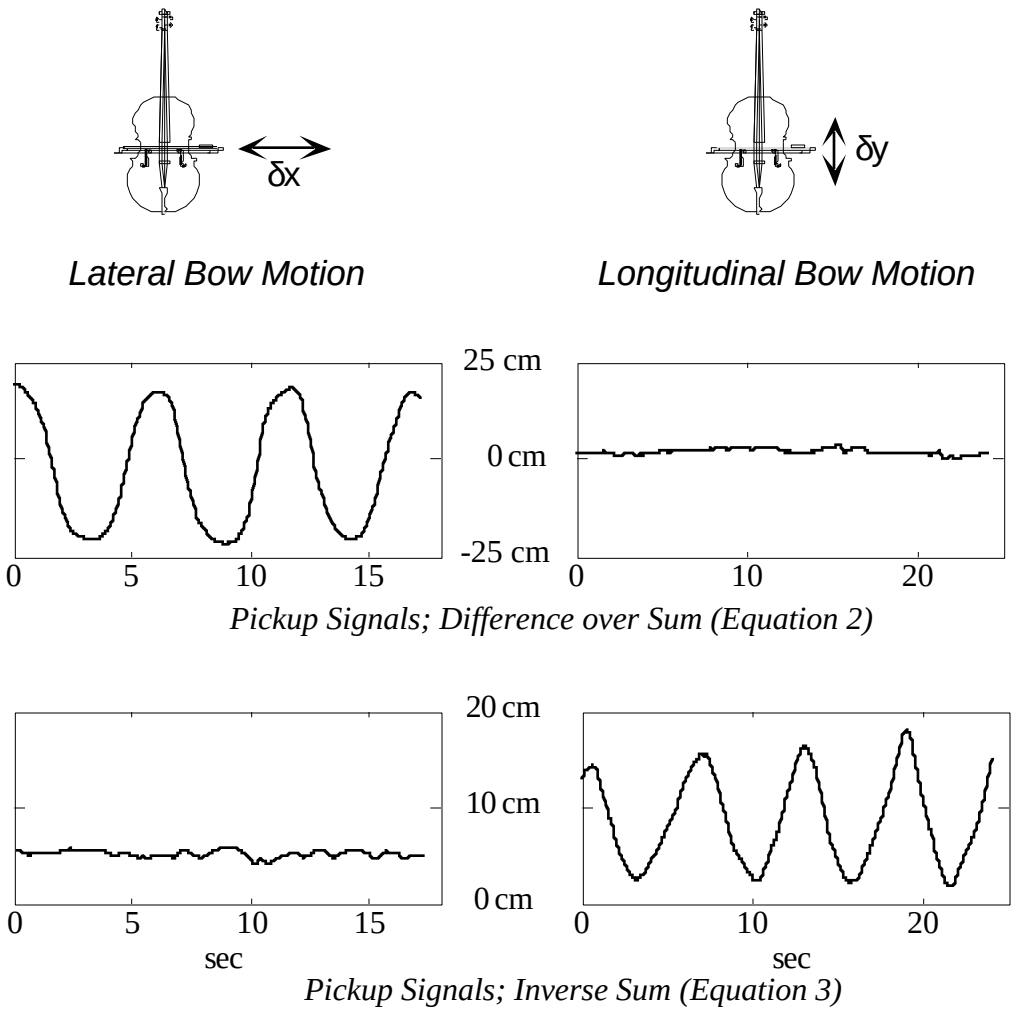

Figure 9: Data from axial and transverse cello bow strokes

1-mm displacement. With sufficient care, such a system can even be extended to measure micron displacements over centimeter ranges [Paradiso and Marlow 1994]. Because of the lack of symmetry in the antenna geometry, it is not possible to exactly solve for C_a (i.e., y) analytically; therefore, in practice, polynomials were fit to experimental measurements to convert the currents into positions. These fits were very close to linear, as predicted by Equations 2 and 3.

The other important degree of freedom in bowing is the pressure. In order to avoid interfering with the bow by measuring this directly from strain in the mounting of the bow hair [Askenfelt 1986], the force applied to the bow was measured under the player's fingers where it is applied. Since there are no thin compression force sensors available commercially with the required sensitivity and response time, an elastic capacitor was developed using a thin (35 mil) urethane "Poron" foam[5] with a modulus (9 PSI per 20% deflection) matched to finger forces. This capacitance was measured with the same circuit used for determining bow position (Figure 6).

---

[5] 4701-59-25035-1648, Poron, Rogers, CT.

Figure 10: Yo-Yo Ma performing in concert on the Hypercello

The hypercello has been used in over a dozen concert performances of *Begin Again Again...*; Figure 10 shows Yo-Yo Ma playing the system at the Tanglewood debut on August 14, 1991. This setup was also adapted to track a viola bow, played by the violist Kim Kashkashian for the premiere of Machover's *Song of Penance* with the Los\ Angeles Philharmonic Contemporary Ensemble [Machover 1991b] .

4) Tracking Violin Bows

The cello bow position sensor described in the last section requires cables connected to the bow. These can be brought out without interfering with a cellist, who is always seated, but this is not true for a violinist, who must perform standing up. A completely wireless bow was thus needed for a collaboration with Ani Kevaffian and the St. Paul Chamber Orchestra in a performance of Machover's hyperviolin composition *Forever and Ever* [Machover 1993]. The first attempted modification of the cello bow was to place both a transmit and receive electrode on the violin to sense the perturbation of the field by a passive resistive strip on the bow. This failed because the measurement was dominated by the position of the player's hand (although this accident proved to be very useful for other applications, as will be discussed in the next section). The successful alternative that was developed for the violin bow involved reversing the roles of the components; i.e. transmitting out from the bow and receiving at the violin bridge, as shown in Figure 11.

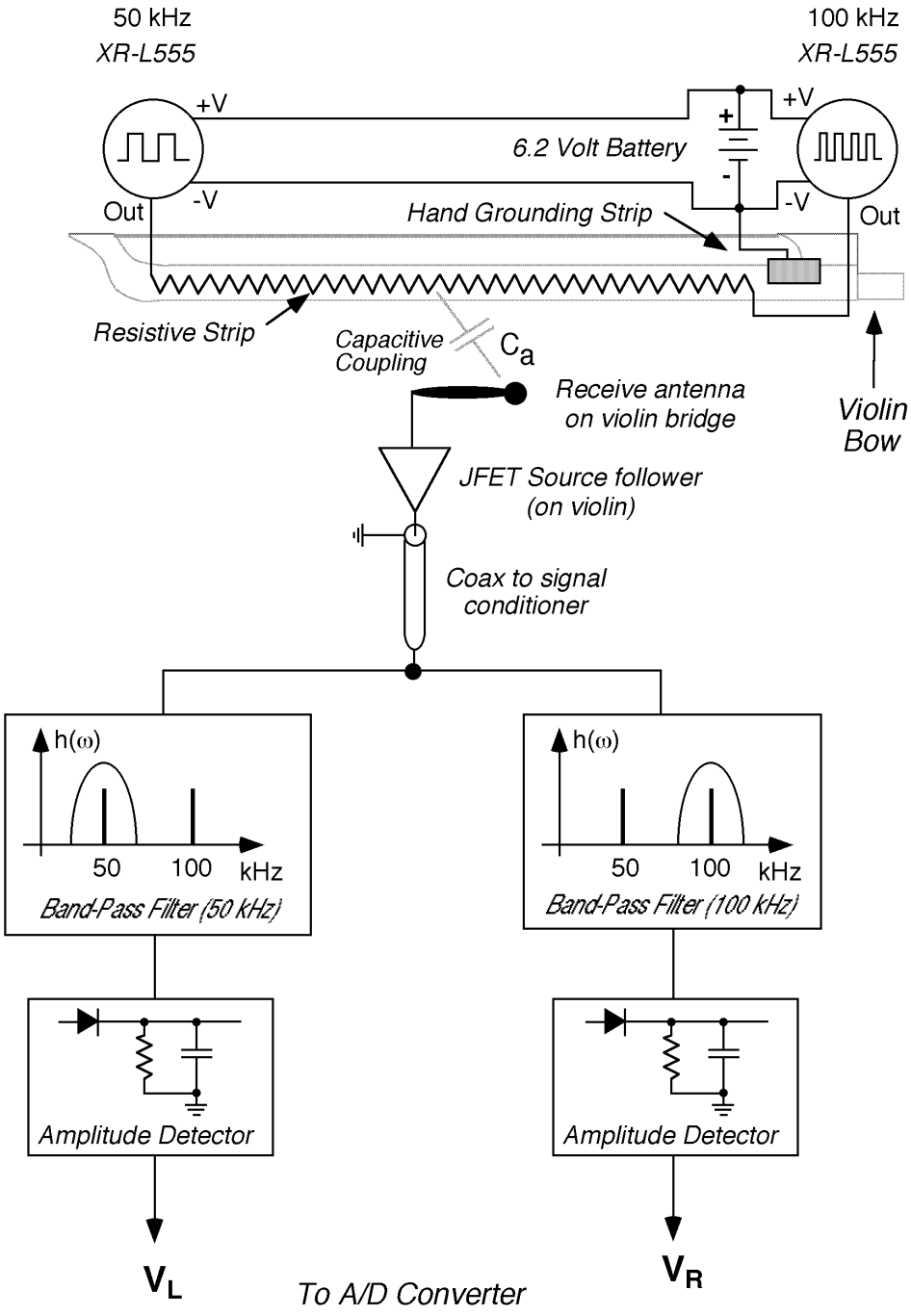

Figure 11: Block diagram of the wireless bow position sensor

Two low-power oscillators using CMOS 555 timer integrated circuits were connected to each end of the resistive strip and tuned to two different frequencies (50 kHz and 100 kHz). The associated circuitry was potted with the chips to make a small, stable, lightweight package that was attached to both ends of the bow. Here, the resistive strip acted as a voltage divider; the proportion of the two frequencies coupled into the bridge antenna varies with the transverse bow position (x). An insulated electrode at the common oscillator ground was placed near the bow frog, where it capacitively couples into the

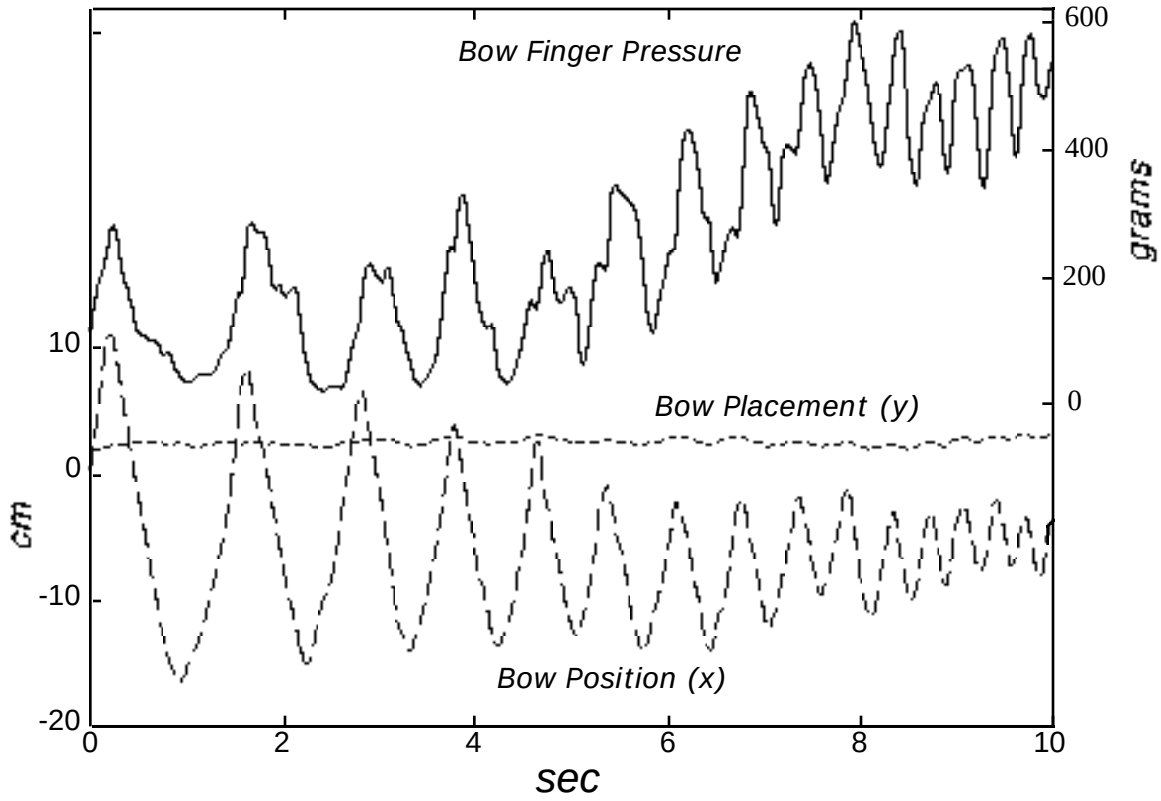

Figure 12: Coordinates and pressure measured by the violin bow sensors

performer's hand to define the system's ground; the performer is also coupled to the receiver ground through a metal foil on the violin that rests against her neck (this kind of coupling can also be exploited for intra-body signaling [Zimmerman 1995]).

The analog signal processing differs considerably from that developed for the cello. An FET source-follower is mounted on the violin, near the bridge antenna. This buffers the received voltage, and drives a 5-meter shielded cable back to the conditioning electronics. Because there is no direct connection between the bow and the conditioning electronics, synchronous detection cannot be used without carrier recovery. Instead, the front-end amplifier is followed by simple second-order bandpass filters; a Q of roughly 6 provided adequate noise rejection for the performance needs. The outputs of the filters were connected to the inputs of envelope followers, which produced voltages corresponding to the amount of signal detected at the frequencies broadcast from the oscillators at each end of the bow. These voltages (v_L, v_R) were then processed to yield estimates of the bow position (x,y), just as described for the cello with (i_L, i_R) in Equations 2 and 3.

To measure the bow pressure, a third CMOS oscillator, running at a different frequency (25 kHz in this case), drove a second antenna running the full length of the bow. The frequency of this oscillator was made to drop with applied pressure. This signal was separated in the receiver from those of the other two oscillators with a fourth-order resonant low-pass filter, then a phased-locked-loop tracked the approximately 3 kHz change in frequency as the bow pressure was varied. Initial implementations used an elastic capacitor, as developed for the cello, in the oscillator timing loop. This solution was not reliable in this circuit, however, as the sensor capacitance (and its change with pressure)

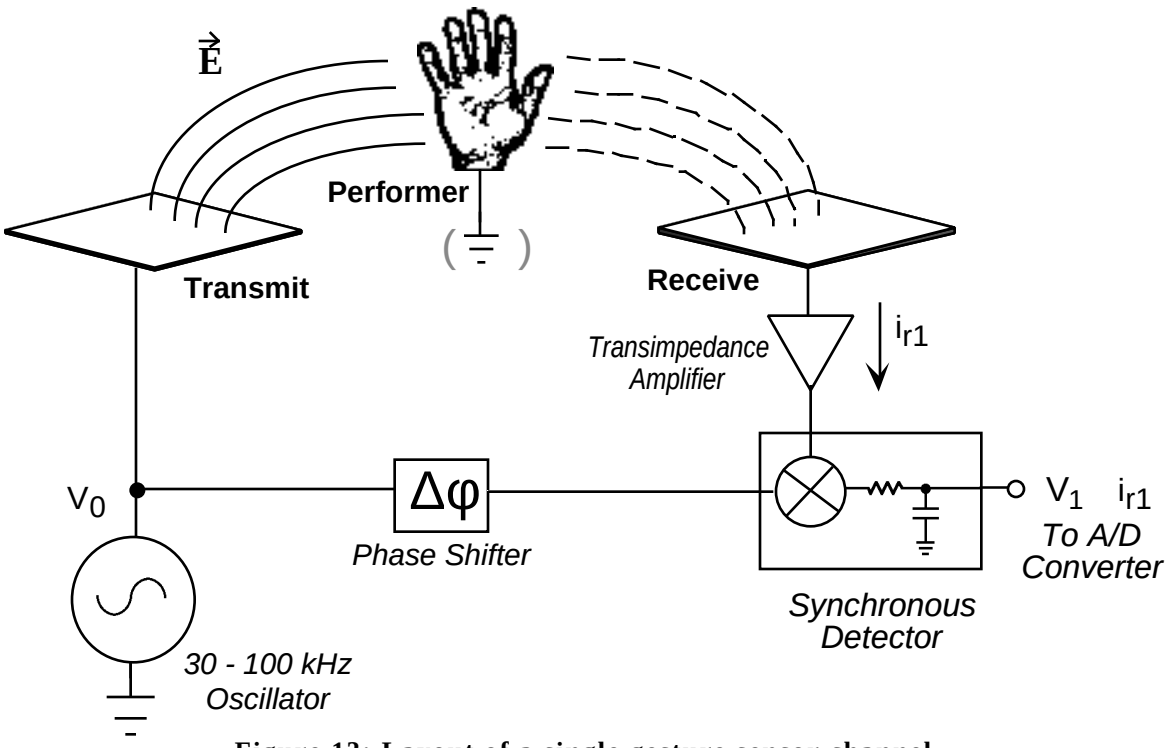

Figure 13: Layout of a single gesture sensor channel

was small, causing drift and mode-locking problems in the oscillator. Instead, a flat, piezoresistive strip from Interlink Electronics (Camarillo, California, USA) was trimmed to fit on the bow and mounted at the location where the index finger is placed. The piezoresistor was used in a simple resistive divider to create a low-impedance voltage that varied with applied pressure and was used to control the oscillator frequency. Although composite piezoresistors have significantly lower resolution than capacitive sensors, this system produced adequate response, as noted in Figure 12, which shows the reconstructed bow coordinates (per Equations 2 and 3) and measurement of applied finger pressure for a violinist using this bow to execute a slow-to-fast dètachè. The applied pressure is seen to cycle with each bow stroke and generally increase at the conclusion of the phrase, as the player's grip tightens while the phrase accelerates and the bowing excursion diminishes.

The three CMOS oscillators are powered from a small six-volt lithium camera battery, mounted on the bow behind the frog. Because all oscillators together draw under two milliamperes of total current, the battery provides approximately 80 hours of constant operation. This system, while usable, does modify the playing characteristics of the bow, mainly due to the added mass of the battery. To reduce this impact, we are currently researching designs using extremely light, remotely powered, passive position sensors.

5) Tracking Body Gesture: Background

Figure 13 shows the geometry that we implemented when attempting to remotely detect a resistive strip on a violin bow, as described earlier. We had hoped that the dynamic presence of the real impedance from the bowed strip would measurably perturb the static complex impedances between electrodes. Instead, the signal was extremely sensitive to the position of the player's hand, and had little to do with the bow. Further,

the sign of the effect was opposite from what would be naively expected. Bringing a dielectric into the field increases the measured displacement current, because more charge is needed on the plates to polarize the dielectric for a given voltage. Similarly, bringing a conductor into the field increases the displacement current, because it effectively brings the plates closer together. The hand is a conducting dielectric, yet inserting the hand into the field has the opposite effect: the displacement current goes down. Experimenting with hamburger in a glove (to make a hand with a detachable arm [Zimmerman 1995]) quickly reveals the explanation: the body is inhomogeneously in the field, and the AC coupling into the room ground is strong enough for it to be able to screen the receiver.

Figure 14 shows this in more detail. Before the body comes into the field, there are field lines going from the transmitter to the receiver. The associated capacitance C_0 ranges from femto- to picofarads (fF to pF) for cm-scale electrodes. Once part of the body is in the field, some field lines go into the body (C_t), some go from the body to the receiver (C_r), and some go from the body out to everything in the environment that is effectively grounded (C_g). In addition, free and bound charge in the body leads to frequency-dependent real and complex internal impedances.

The crucial point to appreciate is the relative magnitude of these effects. C_t and C_r are typically comparable to C_0, again ranging from fF to pF. C_g, on the other hand, is much larger, typically many pF. This includes field lines from the body going out to any pathway coupled to the environment's ground; this can include cables, monitor cases, reinforcing beams, and furniture. Since the resistivity of the vascular system and moist body tissue is low (a few hundred ohms), the body can be considered internally to be a perfect conductor on these scales (although we are studying applications of the small deviations from this good approximation). The potential of the body, then, is given by the current flowing through it, dropped across the impedance of the ground return.

If C_g is much larger than C_t and C_r, the body becomes effectively grounded, and it screens the field. It is then a good approximation to take the reduction in current measured at the receiver to be the electric field strength integrated over the cross-sectional area of the body, weighted by the strength of the ground return (we call this "shunt" mode). This observation has many implications. One transmit/receive pair measures distance, since the field strength (hence signal) falls off as a dipole ($1/r^3$) normal to the electrodes; this gives us a single proximity-sensing channel. However, a pair of electrodes can't distinguish between a large mass far away and a small mass nearby, or recognize a change in the ground return strength. Two receivers with differing length scales break this degeneracy, or for a mass of fixed size, give the 2-D position, allowing a free hand to be used as a joystick or computer mouse. Adding a third electrode distinguishes between rotations and translations in a 2-D measurement, or gives the 3-D position for a fixed-size mass, enabling the hand to be used as a 3-D pointing device [Smith 1996]. In general, for any collection of electrodes there is an ambiguity class of object distributions which cannot be distinguished; enough electrodes must be used to determine the desired number of independent degrees of freedom, opening up a continuum from 1-D sliders to 3-D imaging. In order to explore these possibilities, we have constructed a programmable electrode array, which can dynamically transmit and receive from 16 different locations. This device is now being used to research 3-D tomographic reconstruction of objects in the sensor fields [Smith 1995].

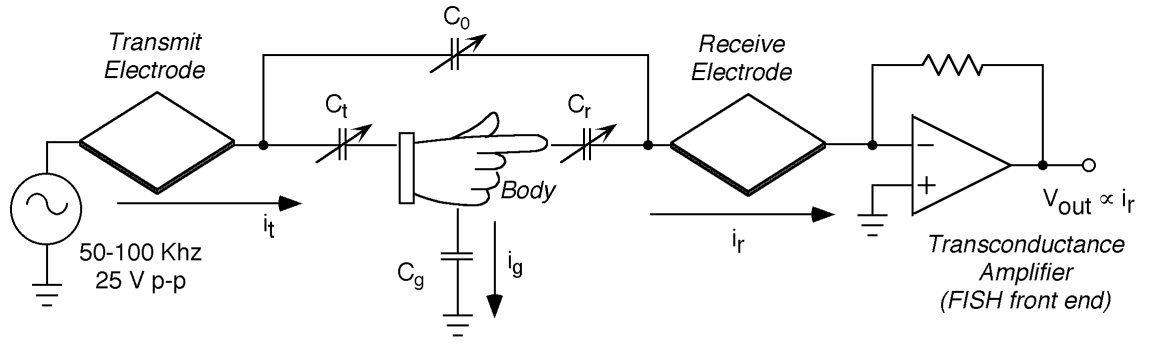

Equivalent circuit for all modes of electric field sensing

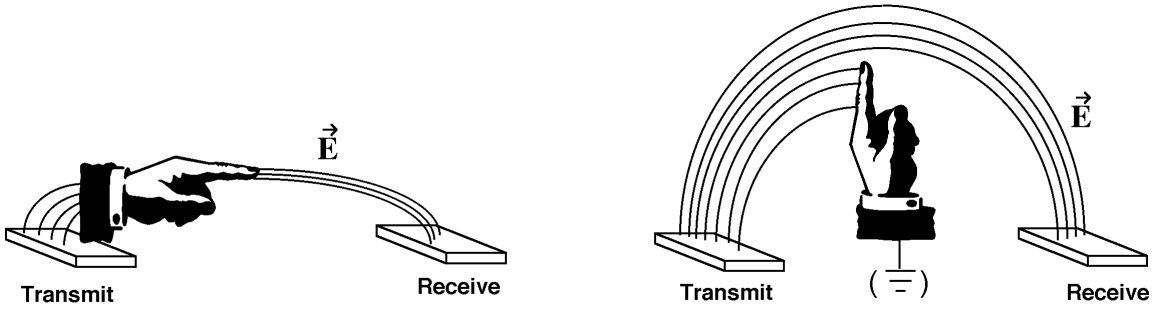

Transmit mode ($C_t >> C_g$)

Shunt mode ($C_g >> C_t$)

Figure 14: Equivalent circuit and modes of operation for electric field sensing

The length scale over which shunt mode can be used is set by the longest distance between transmitter and receiver (although with sufficient averaging, it is possible to make measurements at a few times this distance). Since the transmitter is a fixed voltage source, and the receiver is a virtual ground (up to deviations from ideal behavior in the op-amp and cable), a ground plane can be placed under the transmitter and receiver without influencing the measurement, provided that transmit and receive electrodes are sufficiently close together (otherwise the ground plane shunts away significant transmit flux, attenuating the received signal). This technique allows the electrodes to be shielded in one direction. For example, a set of electrodes can be used on a grounded surface or tabletop, sensing above but not below. As with the bow electronics, each channel can be made for a few dollars in parts, and can remotely measure millimeter displacements of a person on millisecond time scales. Unlike familiar alternatives for finding people (as outlined in the introduction, e.g., ultrasound, video, infrared), this fast and inexpensive measurement is independent of the familiar artifacts from surface texture, orientation, illumination, or ambient environment. Note that these voltages and frequencies are orders of magnitude from any health or regulatory concerns; their effect is comparable to running headphone cables near the body.

There is an important distinction between this shunt mode and the loading mode used in a Theremin. With shunt mode, known boundary conditions are set by the transmit/receive geometry. The distance between the electrodes, and hence the length scale of the field, is known and can be varied by using multiple transmitters or receivers. A set of

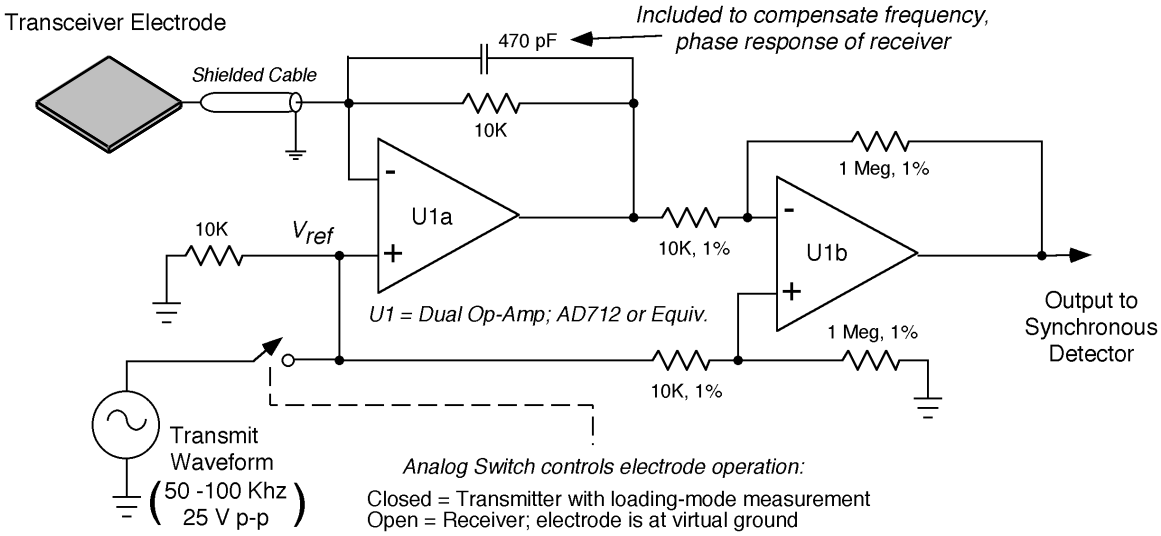

Figure 15: A transceiver electrode

N electrodes thus provide N(N-1)/2 independent shunt measurements. In loading mode, the unperturbed field lines go to unknown boundary conditions in the room, and N electrodes can be used only for N independent measurements. In this sense, an array of electrodes used for loading mode is like a focal-plane array without optics; an array used in shunt mode can be used for imaging [Smith 1995].

A simple modification of the receiver amplifier (Figure 15) permits it to operate as a receiver or as a transmitter (for loading or shunting mode). If V_{ref} is at ground (switch open in Fig. 15), this circuit is identical to the receiver circuit in Figure 6, except that there are now two gain stages instead of one, which improves bandwidth and stability, while reducing receiver sensitivity to the electrode cable length. On the other hand, if V_{ref} is driven by an oscillator (switch closed) and the feedback impedance dominates the shunt impedance of the sensor cable, the op-amp will keep the transceiver electrode at the oscillator potential, turning the electrode into a transmitter. The differential amplifier, driven by low output-impedance sources, will then measure the current dropped across this feedback resistor, which is proportional to the capacitance loading the electrode, as demonstrated by Vranish [1994]. In loading mode, this is the desired signal from the single-electrode measurement; in shunt mode, the transmitter's signal is measured at a receiver.

At 100 kHz, the circuit of Figure 15 can work as a transmitter or shunt-mode receiver with an electrode connected across several meters of shielded input cable. Although the loading-mode measurement degrades much more quickly with cable length, some sensitivity can be recovered by using an activly driven shield (i.e., connect the input cable's shield to V_{ref} instead of ground). Since this simple circuit becomes very small when fabricated with surface-mount components, such transceiver front-ends can easily be embedded onto the electrodes themselves, entirely removing the input cable and its associated parasitic effects, while providing a low-impedance output that can drive much longer cables back to the demodulation electronics.

If the body is very close to the transmitter so that C_t is much larger than C_g, the body becomes a virtual extension of the transmitter instead of a virtual ground. In this case ("transmit mode"), the signal radiated by the body falls off as a parallel-plate capacitor (1/r)

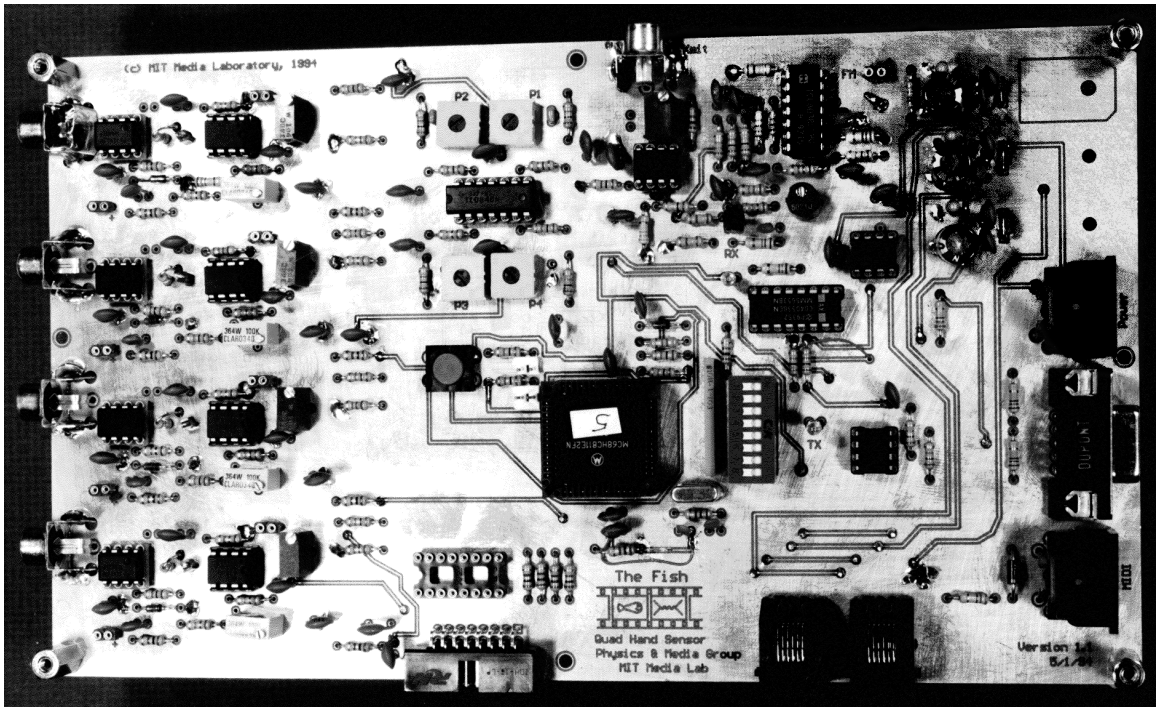

Figure 16: The Fish system (4 channels of synchronous receivers with microcontroller and MIDI output)

when the body is close to the receiver, as a pair of point charges ($1/r^2$) when it is further away, and with an increasingly steeper rolloff as the body moves still further and field lines get diverted to other objects in the environment. Unlike the other two modes (loading and shunting), in transmit mode it is possible to uniquely detect one individual out of many by listening for the frequency being emitted from the connected person's body. This tagging spreads to other people when they are in direct physical contact with the transmitting person and likewise become part of the antenna; the receivers will also respond to their gesture. Transmit mode does not require a wired connection for the transmitter; a battery-powered transmitter is still useful when asymmetrical field displaces the body's potential relative to the room ground [Zimmerman 1995], as demonstrated in the violin-bow application sketched in Figure 11.

All the field-sensing modes require high-gain, low-noise synchronous current amplifiers. To address many such applications, we designed a board (Figure 16) with a transmitter, four receivers, and a microcontroller (the Motorola 68HC811E2) to digitize the analog signals and communicate through MIDI, RS-232, and RS-485 protocols. This device is called the "Fish," both because weakly electrical fish do a similar kind of sensing [Wickelgren 1996; Bastian 1994], and because our Fish can be used as a 3-D version of its companion in animal nomenclature, a 2-D computer mouse [Smith 1996]. With this system, a surprisingly broad range of user-interface problems reduce to configuring an array of appropriately shaped electrodes [Zimmerman et al. 1995]. Because of the low electrode impedance in shunt and transmit modes, the electrodes can be connected to the Fish board over several meters of shielded cable without severe effect; this feature (difficult in Theremin/loading mode, as noted earlier) frees up many options for electrode placement

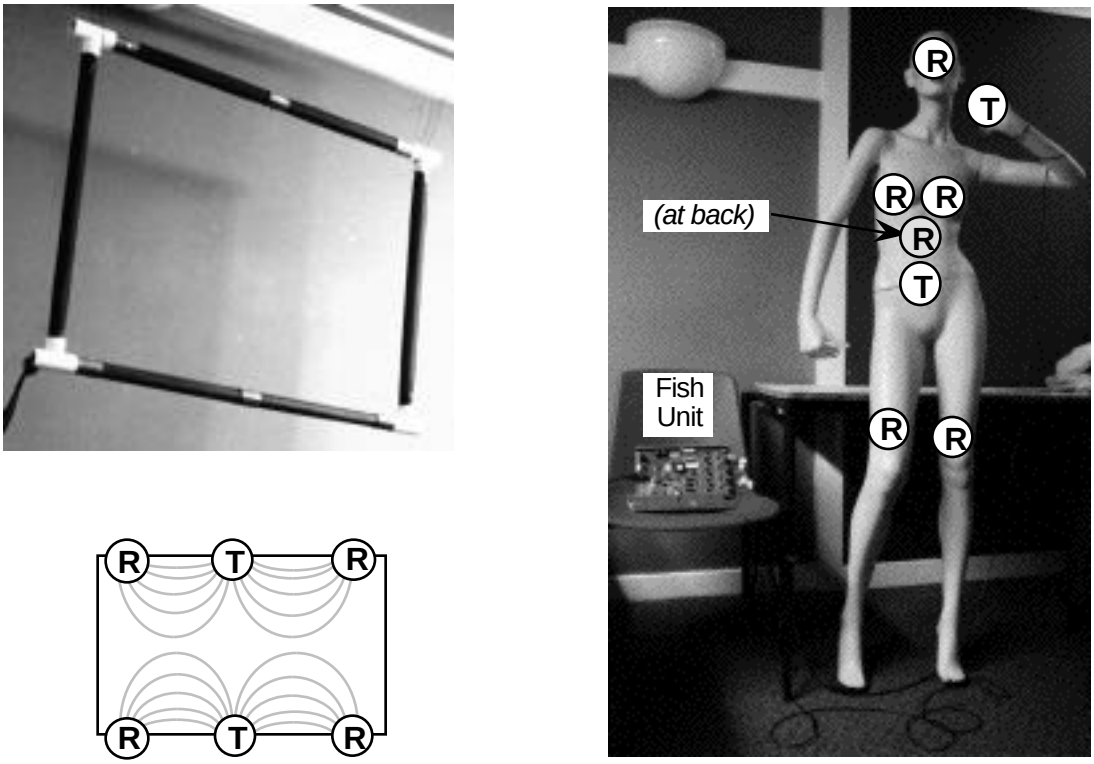

Figure 17: Musical Fish implementations: Gesture Frame and Sensor Mannequin

and layout. We are now developing a successor to this board[6] that doubles the number of channels, turns them into transceivers, eliminates the manual analog adjustments in the front end, increases the resolution from eight to twelve bits, and does all of the signal generation and analysis in a DSP so that algorithms such as synchronous sampling [Vaughan et al. 1991], resolution enhancement by over-sampling, and impulse-response measurement from spread-spectrum autocorrelation, can be implemented.

5) Tracking Body Gesture: Musical Applications

Our work installing sensors on virtuosic acoustic instruments carefully seeks to be constrained by the discipline of past practice. Many other projects at the Media Lab have dispensed with tradition and used the Fish board to build entirely new musical interfaces. The design of these instruments includes both the physical problem of detecting the performer's actions, and the computational and musical problem of designing expressive environments with meaningful mappings from gestures to sounds.

Early applications of the Fish as a musical controller were designed by Waxman, Smith, and collaborators [Waxman 1995]. These included a planar shunt-mode array used for conducting, a large translucent cube (with internal video projection) having sets of hand sensors at two opposing faces to enable a pair of users to control a common sonic

[6] Send electronic mail to *phmreq@media.mit.edu* to inquire about the availability of this board.

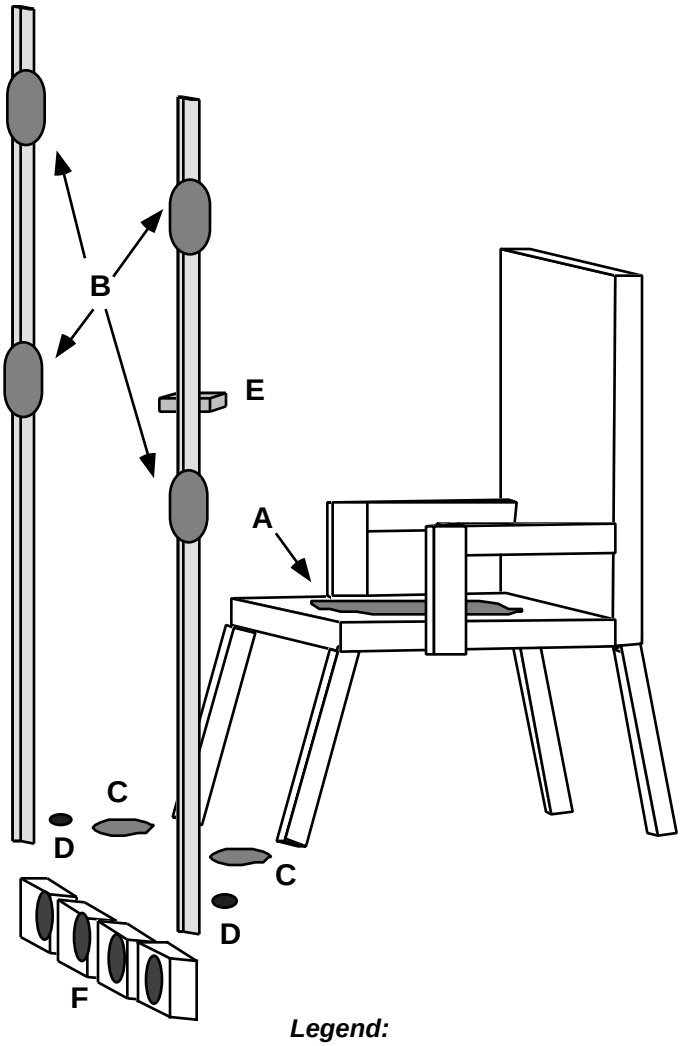

Legend:

A: Copper plate on chair top to transmit 70 kHz carrier signal
B: Four illuminated antennas to sense hand positions
C: Two antennas to detect left and right feet
D: Two pushbuttons for generating sensor-independent triggers
E: Digital display for computer to cue performer
F: Four lights under chair platform, nominally controlled by foot sensors

Figure 18: Layout of the "Spirit Chair"

environment, and a room that responded to the location of occupants by having a transmitter under the floor and receivers on the walls. To address the needs of several music projects, we have designed a general planar structure for shunt-mode hand measurement (the frame shown in Figure 17a) that has transmitters and receivers mounted on 75-cm-long PVC pipes as sketched in the bottom diagram. Duets have been written for pairs of such frames, where the players face one another across these "windows" and collaboratively control algorithms that respond to collective motion [Waxman 1995].

Since the electrodes can sense through insulating materials, they can easily be embedded in other structures to provide a specific visual and/or tactile impression. Perhaps

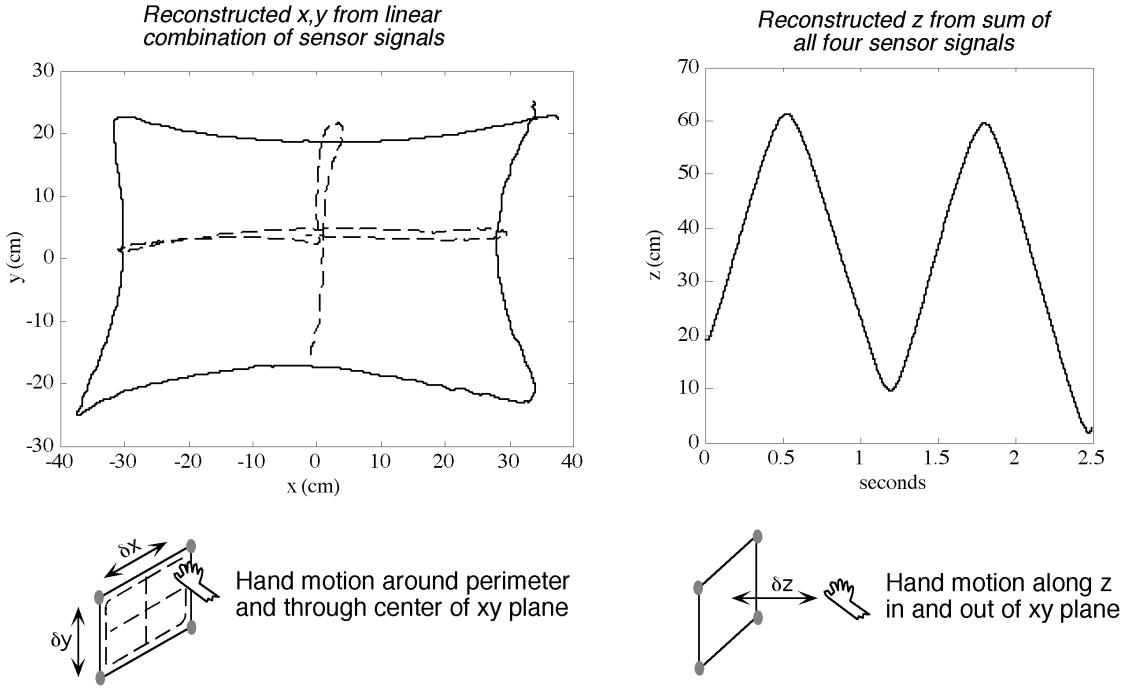

Figure 19: Hand position as linearly reconstructed from spirit chair data

the most unusual such implementation that we have developed (shown in Figure 17b) was in collaboration with the artist formerly known as Prince; a mannequin was embedded with sensor electrodes as labeled, producing musical response to gesture in its vicinity.

None of these examples made absolute position measurements. Instead, they relied on the skills of the player to learn the control mapping, adjusting the electrode shape or the detection parameters where needed to trim the active space. With more care, absolute position measurement is possible, as was realized in the final example to be discussed.

In seances staged near the turn of the century [Tietze 1973], mediums entered "spirit cabinets," where they would supposedly channel supernatural fields from spirits who indicated their presence by making (frequently musical) sounds. With field sensing, it is possible to do that literally (spirits not included), so we designed a modern "spirit chair" for the magicians Penn & Teller, as shown in Figure 18. This was operated in transmit mode because of its selectivity, sensitivity, and simpler coordinate mapping. A copper plate on the chair cushion transmits into the seated performer's body (at about 70 kHz). Four small receiving antennae are mounted at the vertices of a 75 x 50 cm rectangle on poles in front of the chair to monitor the position of the performer's hands, and two electrodes on the floor of the chair platform likewise detect the proximity of the feet. The hand sensors are composed of a copper mesh (the antenna) surrounding a halogen bulb, all enclosed in a 3.5 x 5 cm translucent plastic bottle. The lights (four for the hand sensors and four below the chair platform for the feet) can be independently controlled by MIDI or driven by a voltage proportional to the detected signal strengths, providing visual feedback to the performer and audience.

The rapid, nonlinear decay of the hand signal with distance causes most of the resolution of the 8-bit ADC in the Fish microcontroller to be used very close to the electrodes. A logarithmic amplifier (based on the SSM2100 from Analog Devices) was

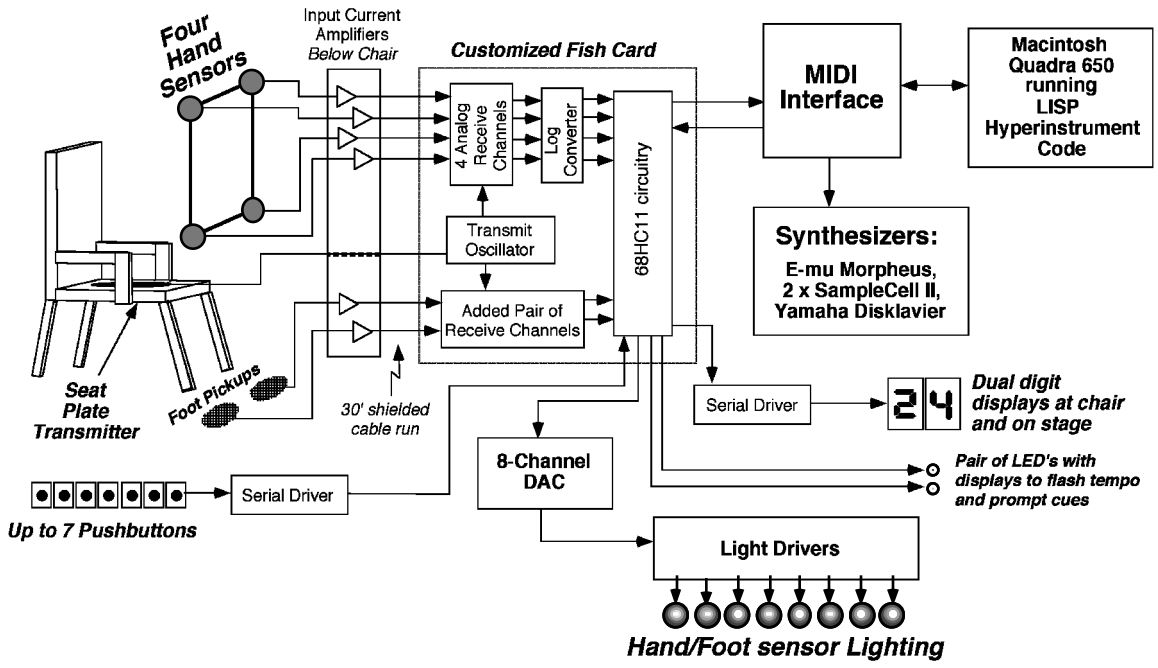

Figure 20: Block Diagram of the spirit chair performance system

therefore inserted between the demodulated hand-sensor receiver outputs and the A/D converter. This very nearly linearizes the signal, and extends the useful gesture range to about three feet (beyond which the performer's body interferes). Because an interpreted software environment was used for this piece (Hyperlisp running on a Macintosh Quadra 650), this hardware linearization was also valuable for reducing the computational burden on the host in estimating the 3-D hand position from the four sensor readings.

Before a performance, readings were taken of the hand position in a 3 x 3 grid (cued by the lights), and a linear least-squares fit was generated to compensate slow changes in the electrostatic environment and any gradual drift in the front-end electronics. Because Penn is so much larger than Teller (their weight ratio is roughly 1.5:1), separate fits were kept for each performer. This worked well: Figure 19 shows the reconstructed position of a hand tracing a grid in real space. The small residual pincushion distortion could be removed by a higher-order fit, but this was unnecessary for the gestural mappings used in the performance. Figure 19 also shows the sum of all four signals for a hand moving in and out normal to the center of the rectangle of receivers; as can be readily noted, this gives a good linear estimate of the hand's distance from the sensor plane.

Figure 20 shows a block diagram of the entire performance system [Paradiso 1994]. The Fish board at its heart has been modified to accommodate six receivers, with log amplifiers on the four hand sensor channels. The 68HC11 microcontroller also accepts MIDI commands for the other interface devices, including eight lighting channels associated with the sensors, a pair of bright LED's on the chair that can be used to indicate tempo, and a two-digit, chair-mounted display to provide performance cues. A pair of footswitches allows sensor-independent triggers, used for explicitly changing parameters in the midst of performance, or instigating triggers when the performer is not seated and hence is unable to use the sensors.

Figure 21: Penn and Teller performing with the spirit chair

As shown in Figure 21, the spirit chair was used in Penn and Teller's performance [Machover 1994a] of Machover's *Media Medium* [Machover 1994b], a mini-opera that integrated the music and chair system into a seance escape trick [Tietze 1973]. The portions of this composition that used the electric field sensors were written as a sequential series of modes with different (and in some cases dynamic) mappings of sonic events and effects onto hand position and motion. Some modes in the piece used the proximity of the performer's hand to the plane of the sensors (z) to launch a sound and adjust its volume, and the position of the hand in the sensor plane (x,y) to change the timbral characteristics. Other modes divided the x,y plane into many zones, which contained sounds and sequences triggered when the hand moved across their boundary. One such mode incorporated 400 percussion sounds distributed evenly across the sensor plane, plus a pair of kick drums on the foot pedals. These triggers were temporally quantized, allowing even an amateur to perform a tight drum solo by waving one's hands and tapping one's feet. Another mode enabled telerobotic control of a Yamaha Disklavier piano; the player could trigger notes by moving a hand forward, with the intensity of the hit determined by the speed of hand motion; foot position controlled the pedals.

As in the seance tricks of yesteryear, public audiences in touring performances often seemed skeptical that the sensor chair was really producing live sound under the control of the performer. Unless one is actually sitting in the chair, it is easy to conclude from observing the generation of sound without obvious connection that the performer is acting along with pre-sequenced music. This is a subtle and recurring problem as gestural sound mappings become complex and the technology gets more "magical"; how important is it for the audience (and even the performer) to understand the causal relationship between what is seen and what is heard?

Although the spirit chair was not intended to be a useful general-purpose computer interface device, its geometry has been applied successfully to information navigation. Mounting the receiving electrodes around a computer monitor enables simple "flying" body gestures to control motion through a virtual environment, producing a very intuitive interface that would be cumbersome with a conventional pointing device [Allport et al. 1995].

6) Conclusions

We have surveyed the three primary modes of applying electric field sensing to people and objects (loading, shunting, and transmitting) and examined their relative strengths and weaknesses. Briefly, loading mode is convenient because it is a single-electrode measurement; shunting mode falls off more quickly with distance, but is better suited to defining sensitive regions and making absolute 3-D measurements; transmit mode is best suited to simple point-tracking applications and can most easily distinguish among multiple objects. Starting with the Theremin, and moving through enhanced string instruments to smart furniture, we have shown that the same relatively simple and inexpensive circuitry can be applied to old and new musical-interface applications that unobtrusively detect a performer's actions at their limiting temporal and spatial resolution. These data can then be mapped into sounds at levels of interaction ranging from simple pitch control to complex shaping of algorithms.

The basic ideas reported here are very old. Although people-sensing applications of capacitive sensing have been known for almost a century, nearly all have been understood and pursued as loading-mode devices. Our experience building new musical interfaces and exploring the underlying physics has helped us to appreciate many different electrical transport mechanisms that were historically lumped together into a category termed capacitance measurement. Pulling these apart has led us to a broad range of new devices, ranging from simple gesture sensors to new techniques for 3-D imaging.

Our hope is that the simplicity and flexibility of interface design with field sensors will help both manufacturers and musicians take a more creative and demanding view of how people control musical instruments. An instrument should be expected to match the physical capabilities of the player, so that the only limitation is the player's intent rather than all-too-familiar hardware deficiencies.

7) Acknowledgments

This research would be impossible without the members of the Physics and Media Group and the thoughtful guidance that comes from our close creative collaboration with Tod Machover and his students. We would also like to thank our tolerant artistic collaborators, particularly Yo-Yo Ma, Penn & Teller, and Ani Kevaffian, and our technical colleagues, including David Allport, Joseph Chung, Rick Ciliberto, Barrett Comisky, Eran Egozy, Ed Hammond, Andy Hong, Theresa Marrin, Pete Rice, Josh Smith, David Waxman, and Tom Zimmerman. We are grateful for support from the members of the Media Lab's *Things That Think* Consortium, and for inspiration from Max Matthews, Bob Boie, and Bob Moog.

8) References

Aikin, J., "Don Buchla," The Art of Electronic Music, William Morrow and Co., NY, 1984, pp. 75-83.

Allport, D., Rennison, E., Straussfeld, L., "Issues of Gestural Navigation in Abstract Information Space," CHI 95: Human Factors in Computing Systems, ACM Press, Denver, Co., 1995, pp. 206-207.

Anderton, C., "STEIM: In the Land of Alternate Controllers," *Keyboard*, Vol. 20, No. 8, August 1994, pp. 54-62.

Askenfelt, A., "Measurement of Bow Motion and Force in Violin Playing," *J. Acoustic Soc. Am*. 80, 1986, 1007-1015.

Azevedo, S. and McEwan, T.E., "Micropower Impulse Radar," *Science and Technology Review*, Lawrence Livermore National Laboratory, January/February 1996, pp. 16-29.

Bastian, J., "Electrosensory Organisms," *Physics Today*, Vol. 47, No. 2, February 1994, pp. 30-37.

Chabot, X., "Gesture Interfaces and a Software Toolkit for Performance with Electronics," *Computer Music Journal*, Vol. 14, No. 2, 1990, pp. 15-27.

Chafe, C., CCRMA, Stanford, CA, Personal Communication, April 1995.

Chung, J., "Hyperlisp Reference Manual," MIT Media Laboratory Technical Report, Music and Cognition Group, 1988.

Collinge, D.J. and Parkinson, S.M., "The Oculus Ranae," *ICMC Proceedings*, 1988, pp. 15-19.

Duperray, J.L., "Les Nouveaux Violons," *Diapason*, No. 296, July-August 1984, pp. 88-89.

Fisher, C.R. and Wilkinson, S., "DIY: Build the EM Optical Theremin," *Electronic Musician*, Vol. 11, No. 5, May 1995, pp. 58-64.

Franklin, R. and Fuller, F., "Electronic Wall Stud Sensor," US. Patent No. 4099118, July 4, 1978.

Galeyev, B.M., "L.S. Termen: Faustus of the Twentieth Century," *Leonardo*, 24(5):573-579, 1991.

Garner, L., "For that Different Sound, Music *a'la* Theremin," *Popular Electronics* Vol. 27, No. 5, November 1967, pp. 29-33,102-103.

Gehlhaar, R., "SOUND=SPACE: an Interactive Musical Environment," *Contemporary Music Review*, Vol. 6, Part 1, 1991, pp. 59-72.

Gershenfeld, N., "Sensors for Real-Time Cello Analysis and Interpretation," *Proc. of the 1991 ICMC*, Montreal, Canada, 1991, p. 151.

Gershenfeld, N., "Method and Apparatus for Electromagnetic Non-Contact Position Measurement With Respect To One Or More Axes," US Patent No. 5,247,261, Sept. 21, 1993.

Hong, A., "Non-linear Analysis of Cello Pitch and Timbre," MS Thesis, Massachusetts Institute of Technology, September 1992.

Jackson, J.D., Classical Electrodynamics, Wiley, New York, 1975.

Lancaster, D., CMOS Cookbook; Second Edition, Sams; Prentice Hall Computer Publishing, Carmel, Indiana, 1988, pp. 332-336.

Machover, T., *Begin Again Again...*, musical score, Ricordi, Milan/Paris, 1991(a).

Machover, T., *Song of Penance*, Ricordi, Milan/Paris, 1991(b).

Machover, T., "Hyperinstruments: A Progress Report," available from the Media Laboratory, Massachusetts Institute of Technology, Cambridge, MA., 1992.

Machover, T., *Forever and Ever*, musical score, Ricordi, Milan/Paris, 1993.

Machover, T., *Penn's Sensor Solo and Teller's Finale*, performance at the Digital Expression Symposium, MIT Kresge Auditorium, October 20, 1994 (a).

Machover, T., *Media Medium*, musical score, Ricordi, Milan/Paris, 1994 (b).

Mann, S., "DopplerDanse: Some Novel Applications of Radar," *Leonardo*, Vol. 25, No. 1, 1992, p. 91.

Martin, S., "The Electronic Odyssey of Leon Theremin," Documentary film, Orion Pictures, 1993.

Mathews, M.V., "The Conductor Program and Mechanical Baton," Current Directions in Computer Music Research, MIT Press, Cambridge, MA., 1989, pp. 263-281.

Mathews, M.V., "Three Dimensional Baton and Gesture Sensor," US Patent No. 4980519, Dec. 25, 1990.

Mattis, O. and Moog, R., "Leon Theremin; Pulling Music out of Thin Air," *Keyboard*, Vol. 18, No. 2, February 1992, pp. 46-54.

McMillen, K., Wessel, D.L., Wright, M., "The ZIPI Music Parameter Description Language," *Computer Music Journal*, 14(4), 1994, pp. 52-73.

Moog, R.A. and Rhea, T.L., "Evolution of the Keyboard Interface: The Bösendorfer 290 SE Recording Piano and the Moog Multiply-Touch-Sensitive Keyboards," *Computer Music Journal*, 14(2), 1990, pp. 52-60.

Moog, R., "Theremin Virtuoso, Clara Rockmore, Recollections of Genius," *Keyboard*, Vol. 20, No. 2, February 1994, pp. 58,69-70,184.

Moog, R., "Build the EM Theremin," *Electronic Musician*, Vol. 12, No. 2, February 1996, pp. 86-100.

Nègyesy, J. and Ray, L., "Zivatar: A Performance System," in M.V. Mathews, J.R. Pierce ed. Current Directions in Computer Music Research, MIT Press, Cambridge, MA, 1989, pp. 283-289.

Newcomb, M.J., The Museum of Synthesizer Technology, PO Box 36, Ware, Herts, UK, July 1994, pp. 89-92.

Paradiso, J.A. and Marlow, D., "Electronics for the Precision Alignment of the GEM Muon System," *Proc. of the 1994 Electronics for Future Colliders Conference*, LeCroy Corporation, Chestnut Ridge, NY, May 1994, pp. 235-249.

Paradiso, J.A., "Penn and Teller Seance Electronics," Physics and Media Group Report, MIT Media Lab, Dec. 1994.

Puckette, M., "Combining Event and Signal Processing in the MAX Programming Environment," *Computer Music Journal* 15(3), pp. 68-77, 1991.

Rich, R., "Buchla Lightning MIDI Controller," *Electronic Musician*, Vol. 7, No. 10, October 1991, pp. 102-108.

Roads, C., The Computer Music Tutorial, MIT Press, Cambridge, MA, 1996, pp. 617-658.

Rockmore, C., The Art of the Theremin, CD on Delios International, Santa Monica, CA, 1987.

Rubine, D. and McAvinney, P., "Programmable Finger-tracking Instrument Controllers," *Computer Music Journal*, Vol. 14, No. 1, 1990, pp. 26-41.

Shapiro, G. and Patterson, W., "From the Yellow Castle," research at Brown University and performances at the Automation House, New York City, April 1972.

Simonton, J., "Build This Theremin," *Electronics Now*, Vol. 67, No. 2, February 1996, pp. 31-32,56-59.

Slater, M., "Universal Serial Bus to Simplify PC I/O," *Microprocessor Report*, Vol. 9, No. 6, pp. 1,6-9, April 17, 1995. See also *http://www.teleport.com/~USB/*.

Smith, J.O., "Physical Modeling Using Digital Waveguides," *Computer Music Journal* 16(4), 1992, pp. 74-91.

Smith, J. R., "Toward Electric Field Tomography," MS Thesis, Massachusetts Institute of Technology, Summer 1995.

Smith, J.R., "Field Mice: Extracting Hand Geometry from Electric Field Measurements," to appear in *IBM Systems Journal*, 1996.

Tietze, T.R., Margery, Harper & Row, New York, 1973.

Vail, M., "EMS VCS3 & Synthi A/AKS," Vintage Synthesizers, Miller Freeman Books, San Francisco, CA, 1993, pp. 102-106.

Vaughan, R.G., Scott, N.L., White, D.R., "The Theory of Bandpass Sampling,"*IEEE Transactions on Signal Processing*, Sept. 1991, 39 (9), pp.1973-84.

Vranish, J.M., "Capaciflector Camera," *NASA Tech Briefs*, 18(10), pp. 58-62, October 1994.

Waxman, D., "Digital Theremins: Interactive Musical Experiences for Amateurs using Electric Field Sensing," MS Thesis, Massachusetts Institute of Technology, Summer 1995.

Weigend, A. and Gershenfeld, N., ed. Time Series Prediction: Forecasting the Future and Understanding the Past, Santa Fe Institute Studies in the Sciences of Complexity, Addison-Wesley, Reading, MA, 1993.

Wickelgren, I., "The Strange Senses of Other Species," *IEEE Spectrum*, Vol. 33, No. 3, March 1996, pp. 32-37.

Wren, C.R, Sparacino, F., et al., "Perceptive Spaces for Performance and Entertainment: Untethered Interaction using Computer Vision and Audition," MIT Media Lab Perceptual Computing Report TR#372, Submitted to Applied Artificial Intelligence (AAI) Journal, Special Issue on Entertainment and AI/ALife, March 1996.

Zimmerman, T.G., "Personal Area Networks (PAN): Near-Field Intrabody Communication," Masters Thesis, MIT, June 1995.

Zimmerman, T.G., Smith, J.R., Paradiso, J.A., Allport, D., Gershenfeld, N., "Applying Electric Field Sensing to Human-Computer Interfaces," CHI 95: Human Factors in Computing Systems, ACM Press, Denver, Co., 1995, pp. 280-287.